# Connectivity and Design of Planar Global Attractors of Sturm Type.
## III: Small and Platonic Examples

Bernold Fiedler
Institut für Mathematik
Freie Universität Berlin
Arnimallee 2–6, D–14195 Berlin, GERMANY
fiedler@math.fu-berlin.de
http://dynamics.mi.fu-berlin.de


Carlos Rocha
Instituto Superior Técnico
Avenida Rovisco Pais, 1049–001 Lisboa, PORTUGAL
crocha@math.ist.utl.pt
http://www.math.ist.utl.pt/cam/

version of June 6, 2007

## Abstract

Based on a Morse-Smale structure, we study planar global attractors $\mathcal{A}_f$ of the scalar reaction-advection-diffusion equation $u_t = u_{xx} + f(x, u, u_x)$ in one space dimension. We assume Neumann boundary conditions on the unit interval, dissipativeness of $f$, and hyperbolicity of equilibria. We call $\mathcal{A}_f$ Sturm attractor because our results strongly rely on nonlinear nodal properties of Sturm type.

Planar Sturm attractors $\mathcal{A}_f$ consist of equilibria, of Morse index 0, 1, or 2, and of the heteroclinic connecting orbits between them. The unique heteroclinic orbits between adjacent Morse levels define a plane graph $\mathcal{C}_f$, which we call the connection graph. The 1-skeleton $\mathcal{C}_f^1$ is the closure of the unstable manifolds (separatrices) of the index-1 Morse saddles.

We summarize and apply two previous results [FiRo07a, FiRo07b] which completely characterize the connection graphs $\mathcal{C}_f$ and their 1-skeletons $\mathcal{C}_f^1$, in purely graph theoretical terms. Connection graphs are characterized by the existence of pairs of Hamiltonian paths with certain chiral restrictions on face passages. Their 1-skeletons are characterized by the existence of cycle-free orientations with certain restrictions on their criticality.

We describe all planar Sturm attractors with up to 11 equilibria. We also design planar Sturm attractors with prescribed Platonic 1-skeletons of their connection graphs. We present complete lists for the tetrahedron, octahedron, and cube. We provide representative examples for the design of dodecahedral and icosahedral Sturm attractors.

# 1   Introduction

Based on a Morse-Smale structure, we apply our previous results [FiRo07a, FiRo07b] on the global spatio-temporal dynamics of the following scalar reaction-advection-diffusion equation in one space dimension

(1.1) $$u_t = u_{xx} + f(x, u, u_x).$$

Here $t \geq 0$ denotes time, $0 < x < 1$ denotes space, and we seek solutions $u = u(t, x) \in \mathbb{R}$. To be completely specific we also fix Neumann boundary conditions

(1.2) $$u_x = 0 \text{ at } x = 0, \text{ and } x = 1.$$

Our results will hold analogously, though, for other separated boundary conditions.

For nonlinearities $f = f(x, u, p)$ of class $C^2$, standard theory provides a local solution semigroup $u(t, \cdot) = \mathcal{T}(t)u_0, t \geq 0$, on initial conditions $u_0 \in X$. For the underlying Banach space $X$ we choose the Sobolev space $H^2$, intersected with the Neumann condition (1.2). See for example [Ta79, He81, Pa83] for a general background.

Our main object is the *global attractor* $\mathcal{A} = \mathcal{A}_f$ of the semigroup $\mathcal{T} = \mathcal{T}_f$. We assume

(1.3) $$f \in C^2 \text{ is dissipative.}$$

Here *dissipativeness* requires that there exists a fixed large ball in $X$, in which any solution $u(t, \cdot) = \mathcal{T}(t)u_0$ stays eventually, for all $t \geq t(u_0)$. In particular, solutions exist globally for all $t \geq 0$. For broad surveys on the theory of global attractors we refer to [BaVi92, ChVi02, Ed&al94, Ha88, Ha&al02, La91, Ra02, SeYo02, Te88] and the many references there. The specific attractors arising from our setting (1.1), (1.2) we call *Sturm attractors*.

A Lyapunov function $\mathcal{V}$ of the form

(1.4) $$\mathcal{V}(u) = \int_0^1 a(x, u, u_x)dx$$

which is strictly decreasing along all solutions $u(t, \cdot) = \mathcal{T}(t)u_0$, except at equilibria, induces a *gradient-like structure* of the semigroup $\mathcal{T}(t)$; see [Ze68, Ma78, Ma88]. For nonlinearities $f = f(x, u)$ which do not contain advection terms $u_x$ a well-known explicit form of $a$ is $a(x, u, p) = \frac{1}{2}p^2 - F(x, u)$ with primitive $F_u := f$.

To exclude degenerate cases we assume *hyperbolicity* of all equilibria

(1.5) $$0 = v_{xx} + f(x, v, v_x)$$

of (1.1), with Neumann boundary conditions $v_x = 0$ given by (1.2). As usual, hyperbolicity of $v$ means that the linearized Sturm-Liouville eigenvalue problem

(1.6) $$\lambda u = u_{xx} + f_p(x, v(x), v_x(x))u_x + f_u(x, v(x), v_x(x))u,$$

1

again with Neumann boundary (1.2), possesses only the trivial solution $u \equiv 0$ for $\lambda = 0$. We call the number of positive eigenvalues $\lambda$ the *unstable dimension* or *Morse index* $i = i(v)$ of the equilibrium $v$.

Let $\mathcal{E} = \{v_1, \ldots, v_N\}$ denote the set of all equilibria. Note that $\mathcal{E}$ is finite, by dissipativeness of $f$ and hyperbolicity of equilibria. Morse inequalities, Leray-Schauder degree, or a shooting argument in fact show that $N$ is odd.

Hyperbolic equilibria $v$ come equipped with local *unstable* and *stable manifolds* $W^u(v)$ and $W^s(v)$ of dimension and codimension $i(v)$, respectively.

As a consequence of the Lyapunov functional (1.4), the global attractor $\mathcal{A}$ of (1.1), (1.2) consists entirely of equilibria and *heteroclinic orbits* $u(t, \cdot)$, which converge to different equilibria for $t \to \pm\infty$. See for example the survey [Ra02]. In other words, Sturm attractors $\mathcal{A}$ consist of just all unstable manifolds,

$$(1.7) \qquad \mathcal{A} = \bigcup_{v \in \mathcal{E}} W^u(v).$$

Indeed the $\omega$-limit set of any trajectory in $W^u(v) \backslash \{v\}$ must consist of a single equilibrium different from $v$ itself, due to the gradient-like structure and hyperbolicity. Therefore all non-equilibrium trajectories in $\mathcal{A}$ are heteroclinic.

Our results also use a generalization of the *Sturm nodal property*, first observed by Sturm [St1836] and very successfully revived by Matano [Ma82]. It is for this property, central to the entire analysis in the present paper, that we use the term *Sturm attractor* for the global attractors of (1.1), (1.2). Let $z(u) \le \infty$ denote the number of strict sign changes of $u \in X \backslash \{0\}$. Let $u^1(t, \cdot)$, $u^2(t, \cdot)$ denote any two nonidentical solutions of (1.1), (1.2). Then

$$(1.8) \qquad t \mapsto z(u^1(t, \cdot) - u^2(t, \cdot))$$

is finite, for any $t > 0$, nonincreasing with $t$, and drops strictly whenever multiple zeros $u^1 = u^2$, $u^1_x = u^2_x$ occur at any $t_0, x_0$. See [An88].

The *Morse-Smale property* requires transverse intersections of all stable and unstable manifolds of equilibria, in addition to hyperbolicity and the gradient-like structure. It was a celebrated result of Angenent and Henry, independently, that this Morse-Smale transversality is, not an additional requirement but, a consequence of hyperbolicity of equilibria for Sturm attractors; see [He85, An86]. See also [Fi94, FiRo96, FiRo99, FiRo00, FiSche03, Ga04, Ra02] for further aspects of nonlinear Sturm theory.

Our description of Sturm attractors is based on the *connection graph* $\mathcal{C}_f$ of the global attractor $\mathcal{A}_f$. Vertices of $\mathcal{C}_f$ are the $N$ equilibria $v_1, \ldots, v_N \in \mathcal{E}_f$ of $\mathcal{A}_f$. An edge of $\mathcal{C}_f$ between $v_j, v_k$ indicates the existence of a heteroclinic orbit between equilibria $v_j$, $v_k$ of adjacent Morse indices $i(v_j) = i(v_k) \pm 1$. By Morse-Smale transversality of stable and unstable manifolds, heteroclinic orbits can only run from higher to strictly lower Morse indices. Therefore

2

the connection graph $\mathcal{C}_f$ comes with a natural flow-defined edge orientation: edges can be oriented from higher to lower Morse index. As an aside we already note here that heteroclinic orbits between adjacent Morse levels turn out to be unique, whenever they exist, in the Sturm setting (1.1), (1.2).

We restrict attention to adjacent Morse levels, for the following two reasons. First, Morse-Smale systems possess a *transitivity property* of heteroclinic connections. Let $v_1 \rightsquigarrow v_2$ indicate that there exists a heteroclinic orbit from $v_1$ to $v_2$. Then $v_1 \rightsquigarrow v_2$ and $v_2 \rightsquigarrow v_3$ implies $v_1 \rightsquigarrow v_3$. The proof is based on the $\lambda$-Lemma; see for example [PdM82]. Second and conversely, special to the Sturm setting (1.1), (1.2), suppose $v_k \rightsquigarrow v_0$ with $i(v_k) = i(v_0) + k$. Then there exist further equilibria $v_1, \ldots, v_{k-1}$ such that $i(v_j) = i(v_0) + j$ and $v_k \rightsquigarrow v_{k-1} \rightsquigarrow \ldots \rightsquigarrow v_1 \rightsquigarrow v_0$ connects through successively adjacent Morse levels. This *cascading principle* was first observed in [BrFi89]; see also [Wo02b]. Together, transitivity and cascading imply that our graph $\mathcal{C}_f$ of Morse-adjacent heteroclinic connections settles the question of whether or not there exists a heteroclinic connection, for any pair of equilibria.

Everything observed so far holds without restrictions on the dimension $\dim \mathcal{A} = \max_{v \in \mathcal{E}} i(v)$ of the global Sturm attractor $\mathcal{A}$. From now on, and for the remainder of this paper, we restrict our attention to the *planar* case $\dim \mathcal{A} = 2$ which only features equilibria $v$ which are *sinks* of Morse index $i(v) = 0$, *saddles* of Morse index $i(v) = 1$, and *sources* of Morse index 2. As a simplified variant of the full connection graph $\mathcal{C}_f$ we also consider its undirected 1-*skeleton* $\mathcal{C}_f^1$. Vertices of $\mathcal{C}_f^1$ are the sink equilibria, only. Edges of $\mathcal{C}_f^1$ are the unstable manifolds $W^u(v)$ of the saddles. More precisely, sink vertices $v_j$, $v_k$ of $\mathcal{C}_f^1$ are connected by an (undirected) edge if, and only if, there exists a saddle equilibrium $v$ such that $v \rightsquigarrow v_j$ and $v \rightsquigarrow v_k$. The 1-skeleton $\mathcal{C}_f^1$ thus ignores sources $w$ in $\mathcal{C}_f$, with $i(w) = 2$, along with their emanating heteroclinics to saddle targets.

Planarity of the connection graphs $\mathcal{C}_f$, $\mathcal{C}_f^1$ does not come as a surprise, for two-dimensional Sturm attractors $\mathcal{A}_f$. In fact it has been noted by [Br90, Ro91] that any $L^2$-orthogonal projection $P$ of any $n$-dimensional Sturm attractor $\mathcal{A}_f$ onto the span of the first $n$ eigenfunctions of any Sturm-Liouville eigenvalue problem (1.6) is injective. Moreover, $\mathcal{A}_f$ becomes a $C^1$ graph over the span. More specifically, the zero number satisfies

$$(1.9) \qquad z(u_1 - u_2) < \dim \mathcal{A}_f = \max_{\mathcal{E}_f} i(v)$$

for any two distinct elements $u_1$ and $u_2$ of $\mathcal{A}_f$. For planar Sturm attractors, we will therefore identify the connection graph with the unique heteroclinic orbits between equilibria of adjacent Morse levels, via the planar embedding $P$.

We now state the two main results from [FiRo07a, FiRo07b]. For the convenience of the reader we also summarize some graph terminology. We exclude the case of a trivial Sturm attractor $\mathcal{A}_f$ which consist of only one single globally attracting equilibrium.

3

**Theorem 1.1** *A graph $G$ is the 1-skeleton $\mathcal{C}_f^1$ of the connection graph $\mathcal{C}_f$ of some at most two-dimensional nontrivial Sturm attractor $\mathcal{A}_f$ with only hyperbolic equilibria if, and only if, $G$ satisfies the following two properties:*

   *(i) $G$ is a finite, connected, plane, cellular multigraph without loops, and*

   *(ii) $G$ possesses an orientation with exactly one di-sink $\bar{v}$ and one di-source $\underline{v}$, both on the boundary $\partial G$, and without di-cycles.*

*Moreover $\partial G$ is oriented from $\bar{v}$ to $\underline{v}$.*

**Theorem 1.2** *A graph $G_2$ is the connection graph $\mathcal{C}_f$ of some nontrivial, at most two-dimensional Sturm attractor $\mathcal{A}_f$ with only hyperbolic equilibria if, and only if, $G_2$ satisfies the following two properties:*

   *(i) $G_2$ is the filled graph of a finite, connected, plane, cellular multigraph $G$ without loops, and*

   *(ii) $G_2$ possesses a boundary ZS-Hamiltonian pair $(h_0, h_1)$ which starts and ends at two distinct vertices $\underline{v}$, $\bar{v}$ in the boundary $\partial G$.*

*Moreover the "flow" directed filled graph $G_2$ then coincides with the flow directed connection graph $\mathcal{C}_f$.*

We review our terminology, next. See also [BeWi97], section 1.6 and 11.2. We call a graph $G$ *plane*, $G \subseteq \mathbb{R}^2$, if its vertices $v_j$ and edges $e_{jk} = \{v_j, v_k\}$ are embedded in the plane as points and continuous curves, respectively, such that edges neither intersect nor self-intersect, except possibly at their vertex end points $v_j$, $v_k$. A *loop* is an edge $\{v_k, v_k\}$ with identical end points $v_k$. A *multigraph* is allowed to possess several edges $e_{jk}^\ell$ connecting the same pair of vertices $v_j$ and $v_k$. Rather than assigning an integer weight to a single edge, we represent multiple edges by multiple nonintersecting curves sharing the same end point vertices. A multigraph $G$ is *finite*, if it consists of finitely many vertices and edges. Any finite plane multigraph $G$ decomposes the complement $\mathbb{R}^2 \backslash G$ into finitely many connected components called *regions* or *faces* of $G$. Exactly one of the regions is unbounded, and its boundary vertices and edges are called the *boundary $\partial G$* of $G$.

For finite connected, plane multigraphs with $N$ vertices, $m$ edges and $r$ bounded faces we recall the Euler characteristic

(1.10) $$N - m + r = 1.$$

A path traverses any sequence $e_{k_0 k_1}^{\ell_1}$, $e_{k_1 k_2}^{\ell_2}, \ldots, e_{k_{r-1} k_r}^{\ell_r}$ of distinct multi-edges via distinct vertices. In the exceptional case $k_0 = k_r$ where the first and last vertex only are allowed to
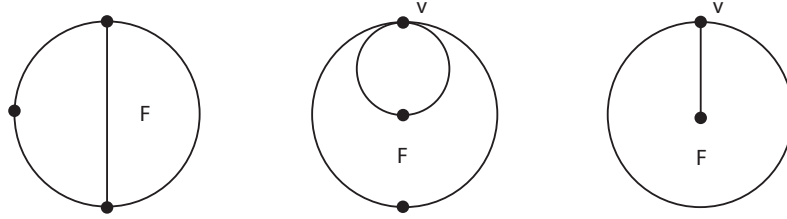
Figure 1.1: Cellular and non-cellular multigraphs. Left: cellular. Center: not cellular (doubly traversed vertex $v$ on face boundary $F$). Right: not cellular (doubly traversed edge on face boundary).

coincide, a path is called a *cycle* or *closed*. A (not necessarily closed) path which visits each vertex exactly once is called a *Hamiltonian path*. A *Hamiltonian cycle*, similarly, is a cycle which is a Hamiltonian path.

We call a plane multigraph *cellular* if each of its (bounded) faces $F$ is bounded by an (undirected) cycle of distinct edges and vertices. See figure 1.1 for illustration. In other words, each bounded face $F$ is the interior of a plane (topological) $n$-gon, for some $n \geq 2$. In particular, the closure of each bounded face is homomorphic to a 2-disk.

Each boundary edge $e \subseteq \partial G$ is the boundary of at most one bounded face. Each other edge, called *interior*, is in the boundary of exactly two bounded faces. We note a slight asymmetry in the role of the unbounded face. Under compactification of $\mathbb{R}^2$ to the 2-sphere $S^2$, the previously unbounded open face will be homomorphic to an open 2-disk but will not necessarily become a cell of the resulting graph on $S^z$. The simplest connected example is the graph $G$ of two vertices, $v_1$, $v_2$ with a single edge joining them.

To say that one plane graph $G$ "is" another plane graph $\tilde{G}$ indicates an *isomorphism*. The standard notion of graph isomorphism is a vertex bijection which preserves edges. For our plane graphs, we require a homeomorphism of the plane graph, including its bounded faces, which maps edge curves to edge curves and vertices to vertices. Combinatorially, it is sufficient to preserve face boundaries, in addition to the usual notion.

As a variant, we call directed (or, oriented) multigraphs *orientation isomorphic*, if the above isomorphism also respects their given orientations.

*Directed* (or, oriented) multigraphs come with an orientation, for each edge. Directed paths, directed Hamiltonian paths, and di-cycles (i.e., directed cycles), are required to traverse edges in the given direction. A vertex $\underline{v}$ of a directed multigraph is called a *directed source* (short: *di-source*) if all its edges point away from it. If all its edges point toward $\bar{v}$, then we call $\bar{v}$ a *di-sink*.

An orientation of $G$ without di-cycles, as in part (ii) of theorem 1.1, equivalently defines a partial order on the vertices of $G$ such that the orientation points downhill. In that sense we may call $\bar{v}$ and $\underline{v}$ the unique minimum and maximum of this order, respectively. This notion differs, in general, from the Morse notion of source and sink equilibria in planar global attractors $\mathcal{A}_f$ based on their Morse index to be 0 or 2, respectively.

The full connection graph $\mathcal{C}_f$ and its flow-oriented variant can both be reconstructed uniquely from their 1-skeleton $\mathcal{C}_f^1$. We detail this construction next, for arbitrary finite, plane, cellular multigraphs $G$ without loops. Motivated by $\mathcal{C}_f$ and its 1-skeleton, we call the vertices of $G$ *Morse sinks*. Starting from $G$, bisect each edge by an additional vertex. Call the bisecting vertices *Morse saddles*. In each (bounded) face, insert one additional vertex and call it a *Morse source*. Draw an edge from each Morse source to the $n$ bisecting Morse saddles on the boundary of its face. We call the resulting undirected graph $G_2$ the *filled graph* of $G$. By construction, $G$ is the 1-skeleton of its filled graph $G_2$. Obviously there is a *"flow" directed* variant of this construction. We just orient bisected edges away from their bisecting Morse saddles, and edges in bounded faces of $G$ away from their Morse sources.

The absence of di-critical vertices from the oriented 1-skeleton $G$, other than the maximal start vertex $\underline{v}$ and the minimal termination vertex $\bar{v}$, is a consequence of the absence of di-cycles; see section 2 in [FiRo07a]. We call a vertex $v$ of a plane directed multigraph $G$ *di-critical*, unless the edges pointing toward $v$ and the edges pointing away from $v$ each form nonempty and non-interspersed sets, when going around $v$ clockwise. In other words, we can traverse a small circle around $v$, say clockwise, such that we first meet all edges oriented toward $v$, and then all edges oriented away from $v$. All equilibria in a plane, flow-oriented connection graph $\mathcal{C}_f$, for example, turn out to be di-critical vertices: sources, sinks, and also, by the geometry of their stable and unstable manifolds in $\mathcal{A}_f$, the saddles. The orientation of the 1-skeleton $G$ in theorem 1.1 above will therefore differ fundamentally from any flow-defined orientation, for which any Morse-sink is a di-sink, for example.

We call a Hamiltonian path $h_0$ in the filled graph $G_2$ a *boundary Z-Hamiltonian path*, if the properties (a)–(c) below all hold. Properties (b), (c) restrict the path $h_0$ as it traverses any Morse source $w$ in a face $F$. Let $\ldots v_{-2}v_{-1}wv_1v_2\ldots$ denote the vertex sequence along $h_0$. Then $v_{\pm 1}$ are Morse saddles on the face boundary $\partial F$. The vertices $v_{\pm 2}$ are Morse sinks, or other Morse sources outside $F$. If $v_{-2}$ or $v_{+2}$ is a Morse sink then it belongs to $\partial F$. Since $\partial F$ contains at least four vertices, and $v_1v_2$ are immediate successors, we can then speak of a clockwise or counter-clockwise direction of the arc $v_1v_2$ from $v_1$ to $v_2$, uniquely, and similarly for $v_{-2}v_{-1}$. Specifically we require

(a) "**Boundary**":

$h_0$ starts at some vertex $\underline{v}$ in the boundary $\partial G$, and terminates at another vertex $\bar{v}$.

6

(b) "**No right turn exit**":

Whenever $h_0 = \ldots w v_1 v_2 \ldots$ exits any Morse source $w$ of a face $F$, then $v_1 v_2$ are not both on $\partial F$ in clockwise direction.

(c) "**No left turn entry**":

Whenever $h_0 = \ldots v_{-2} v_{-1} w \ldots$ enters any Morse source $w$ of a face $F$, then $v_{-2} v_{-1}$ are not both on $\partial F$ in clockwise direction.

The letter $Z$ graphically indicates the admissible behavior, in case both the exit arc $v_1 v_2$, on top, and the entry arc $v_{-2} v_{-1}$, on bottom, are on $\partial F$: right turn entry and left turn exit. Note however, that $h_0$ is also permitted to connect Morse sources of adjacent faces through the bisecting Morse saddle of a shared edge, without creating an arc on $\partial F$ at all. The *reverse path* $h_0^- = \ldots v_2 v_1 w v_{-1} v_{-2} \ldots$ of $h_0$ is boundary $Z$-Hamiltonian, whenever $h_0$ is, albeit with reversed roles of the start and termination points $\underline{v}$ and $\bar{v}$.

By plain reflection $\kappa$ we can also define (*boundary*) *S-Hamiltonian paths* $h_1$. We simply call $h_1$ an $S$-Hamiltonian path for $G_2$ if the reflected path $h_0 := \kappa h_1$ is $Z$-Hamiltonian for the reflected graph $\kappa G_2$. In other words, the $S$-Hamiltonian path $h_1$ is neither permitted right turns, upon face entry, nor left turns upon exit. By a (*boundary*) *ZS-Hamiltonian pair* $(h_0, h_1)$ we mean a $Z$-Hamiltonian path $h_0$ and an $S$-Hamiltonian path $h_1$ in $G_2$, both of which start at the same vertex $\underline{v}$ and terminate at the same, distinct, vertex $\bar{v}$ in $G$. See figure 1.2 for examples.

To design Sturm attractors with prescribed plane connection graphs $G_2$ and 1-skeletons $G$ we proceed as follows. We start from an *admissible orientation* of $G$, i.e., an acyclic orientation with $\underline{v}, \bar{v}$ as the only di-critical vertices. In [FiRo07a] we have shown how such an orientation of $G$ defines unique boundary $Z$- and $S$-Hamiltonian paths $h_0$ and $h_1$ in the filled graph $G_2$, which follow the given orientation on the 1-skeleton $G$. These paths can be interpreted as the ordering of equilibria $v_k$ by their boundary values at $x = 0, 1$, respectively. These orders, in turn, determine the global Sturm attractor $\mathcal{A}_f$. In fact, the 1-skeleton $\mathcal{C}_f^1$ and the connection graph $\mathcal{C}_f$ then coincide with the prescribed 1-skeleton $G$ and its filled counterpart $G_2$, respectively.

In section 2.1 we review the properties of Sturm permutations $\pi := h_0^{-1} \circ h_1$ and recall how they determine Morse indices of equilibria and the connection graph. We discuss trivial attractor equivalences, duality of connection graphs, and the constructions of attractor stacking and face gluing, in sections 2.2–2.5. We also recall the very special case of an $n$-gon connection graph and attractor; see section 2.6 and figure 1.2.

37 planar Sturm attractors with up to 11 equilibria. We also design planar Sturm attractors with prescribed Platonic 1-skeletons of their connection graphs. We present complete lists for
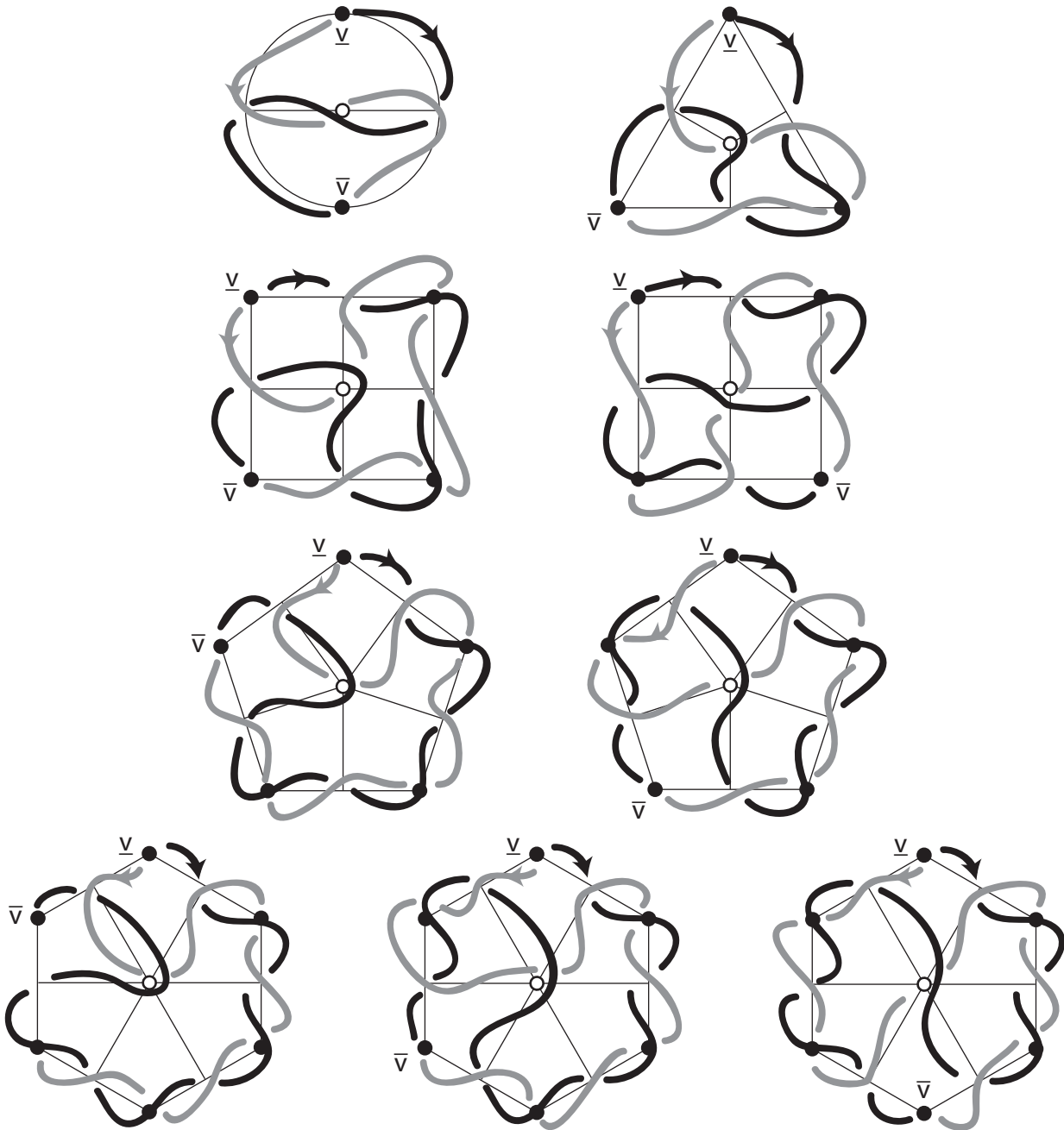
Figure 1.2: Boundary Hamiltonian pairs $(h_0, h_1)$ for $n$-gons, $n = 2, \ldots 6$. Path $h_0$ black, path $h_1$ gray.

the tetrahedron, octahedron, and cube. We provide representative examples for the design of dodecahedral and the icosahedral Sturm attractors.

**Acknowledgments**

# 2  Generalities

In this section we collect several general tools for subsequent use in the design of specific Sturm attractors.

## 2.1  Orientations, Hamiltonian paths, Sturm permutations, and Sturm attractors

We first recall the role of the boundary $ZS$-Hamiltonian pair $(h_0, h_1)$ in the connection graph $\mathcal{C}_f$ and the Sturm attractor $\mathcal{A}_f$. See also [Ra02, FiSche03] for surveys. At the end of this section we formulate a recipe to design Sturm permutations $\pi_f$ from orientations of prescribed 1-skeletons $G$ and from $ZS$-Hamiltonian paths of their filled graphs $G_2$, such that the connection graph and its 1-skeleton indeed coincide with $G_2$ and $G$, respectively.
Our concept of $ZS$-Hamiltonian pairs $(h_0, h_1)$ is motivated, as we have seen in [FiRo07a], by the fact that the ordering of equilibria $v_k$ of the Sturm PDE (1.1), (1.2), alias vertices of the connection graph $\mathcal{C}_f$, by their boundary values $v_k(x)$ at $x = 0, 1$, respectively, defines a pair of $Z$- and $S$-Hamiltonian paths with properties (a)–(c). The hyperbolic equilibria

$$(2.1) \qquad\qquad \mathcal{E}_f = \{v_1, \ldots, v_N\} \subsetneq \mathcal{A}_f$$

are the vertices of the connection graph $\mathcal{C}_f$. On the boundaries $x = 0, 1$, respectively, we define the *boundary permutations* $h_i = h_i^f \in S_N$ by the boundary order

$$(2.2) \qquad v_{h_i(1)}(x) < v_{h_i(2)}(x) < \ldots < v_{h_i(N)}(x), \quad \text{at } x = i = 0, 1.$$

The central object in the classification of Sturm attractors, ever since it was first introduced by Fusco and Rocha in [FuRo91], is the *Sturm permutation* $\pi = \pi_f$ defined by

$$(2.3) \qquad \pi := h_0^{-1} \circ h_1.$$

Relabeling equilibria by any permutation $\sigma \in S_N$ corresponds to replacing $h_i$ by $\sigma \circ h$. This does not affect the Sturm permutation $\pi$. For example we may label the equilibria $v_1, \ldots, v_N$ such that $h_0 = id$ is the identity permutation, and thus $v_1 < v_2 < \ldots < v_N$ at $x = 0$. Then $\pi = h_1$ simply keeps track of the order

$$(2.4) \qquad v_{\pi(1)} < v_{\pi(2)} < \ldots < v_{\pi(N)} \quad \text{at } x = 1.$$

For simplicity of presentation we fix this labeling in the present section.

The Sturm permutations $\pi = \pi_f$ encode geometric and dynamical information on the Sturm attractors $\mathcal{A} = \mathcal{A}_f$ and, in fact, turn the study of their connection graphs $\mathcal{C}_f$ into a combinatorial task. We describe some of these results next, as they have been obtained over the past decades, starting with preliminary results in [ChIn74, CoSm83, He85, BrFi88, BrFi89, HaMi91] for nonlinearities $f = f(u)$.

In [FiRo99] it has been observed that any permutation $\pi \in S_N$ is a Sturm permutation, i.e., $\pi = \pi_f$ for some dissipative nonlinearity $f = f(x, u, u_x)$ with only hyperbolic equilibria, if, and only if, $\pi$ is a *dissipative Morse meander*. We recall these three notions next.

We call a permutation $\pi \in S_N$ *dissipative*, whenever $N$ is odd and $\pi(1) = 1, \pi(N) = N$ are fixed under $\pi$.

We call a permutation $\pi \in S_N$ *Morse*, whenever the following $N$ quantities $i_j$ are all non-negative:

$$(2.5) \qquad i_j := \sum_{\iota=1}^{j-1} (-1)^{\iota+1} \operatorname{sign} \left( \pi^{-1}(\iota + 1) - \pi^{-1}(\iota) \right).$$

Note $i_1 = 0$ by the empty sum.

To define *meanders*, we follow Arnold [ArVi89] and consider a $C^1$ Jordan curve $\mathcal{S}$ which intersects the horizontal axis transversely and at precisely $N$ locations, numbered $k = 1, \ldots, N$ in increasing order. Also number the same intersections successively along the curve $\mathcal{S}$. The second numbering $j$ provides a permutation $j = \pi(k)$, relative to the first. Any permutation $\pi$ arising by such a construction is called meander permutation. See figure 2.1 for an example of a dissipative Morse meander $\pi \in S_{13}$. For many more examples see sections 3 and 4 below. It is fairly straightforward to see that Sturm permutations $\pi = \pi_f$ are dissipative Morse meanders. In fact, $v_1 = \underline{v}$ and $v_N = \bar{v}$ are the lowest and highest equilibria in the global attractor $\mathcal{A}_f$ as discussed in section 1. In particular (2.2), (2.3) imply $\pi(1) = 1$ and $\pi(N) = N$. The Morse property of $\pi$ follows because $i_j = i(v_j)$ are the Morse indices of the equilibria

10

Figure 2.1: Dissipative Morse meander permutations $\pi = (1\ 8\ 9\ 10\ 11\ 12\ 7\ 2\ 3\ 4\ 5\ 6\ 13)$ and shooting curve $\mathcal{S}$. For $k$ below the horizontal axis, $j = \pi(k)$ is denoted above. Filled dots indicate $i_j = 0$ and the circled dot has $i_7 = 2$. For all other intersections, $i_j = 1$.

$v_j$, by [FuRo91, Ro91], and hence nonnegative. Therefore $i_N = 0$ for the top sink $\bar{v} = v_N$, and hence $N$ is odd by (2.5) mod 2 with $j = N$. The meander property follows by shooting: consider the equilibrium second order ODE (1.5) with initial condition $v_x = 0$ given by the horizontal $v$-axis in the $(v, v_x)$ phase plane. The diffeomorphic image of the $v$-axis in the phase plane $(v, v_x)$, at $x = 1$, is called the *shooting curve* $\mathcal{S}$. The curve $\mathcal{S}$ crosses the $v$-axis transversely, at the boundary values $v_j(x)$ of the hyperbolic equilibria evaluated at $x = 1$. The permutation $\pi$ associated to the shooting curve $\mathcal{S}$ is the Sturm permutation defined in (2.3), (2.4) above. Numbers $j$ above the $v$-axis indeed indicate the ordering of equilibria at $x = 0$, i.e., along the shooting curve $\mathcal{S}$, whereas numbers $k$ below the axis indicate their ordering at $x = 1$. This explains why Sturm permutations are dissipative Morse meanders. It is significantly more difficult, but has been established in [FiRo99], that all dissipative Morse meanders $\pi$ are indeed Sturm permutations $\pi = \pi_f$, for some nonlinearity $f$.
In [FiRo00] it has been shown that Sturm attractors $\mathcal{A}_f$ and $\mathcal{A}_g$ are $C^0$ orbit equivalent if their Sturm permutations coincide:

$$(2.6) \qquad\qquad \pi_f = \pi_g \quad \Rightarrow \quad \mathcal{A}_f \cong \mathcal{A}_g.$$

Here $C^0$ orbit equivalence $\cong$ requires that there exist a homeomorphism between $\mathcal{A}_f$ and $\mathcal{A}_g$ which maps orbits of the PDE (1.1), (1.2) under nonlinearity $f$ to orbits under $g$, preserving time direction. As we shall see and discuss below, the converse of (2.6) does not always hold. See figures 3.7, 3.9, 3.11, and sections 2.6 and 4 for specific examples.
The key to our construction of prescribed connection graphs $\mathcal{C}_f = G_2$ from boundary $ZS$-Hamiltonian pairs $(h_0, h_1)$ between $\underline{v}$ and $\bar{v}$ in $G_2$ is the derivation of connection graphs $\mathcal{C}_f$

11

from Sturm permutations $\pi_f = \pi$ *defined* by (2.3). See theorem 1.2 and [FiRo07b]. In fact, such permutations $\pi$ are always dissipative Morse meanders, by construction, and it has been shown in [FiRo96] that any dissipative Morse meander is in fact a Sturm permutation for some suitable nonlinearity $f$. See also the very elegant presentation in [Wo02a].

Let us summarize. To design Sturm attractors with prescribed plane connection graphs $G_2$ and 1-skeletons $G$ we can proceed by the following *recipe*. We first choose an admissible orientation of $G$, i.e., an acyclic orientation with a choice of vertices $\underline{v}, \bar{v}$ on the boundary $\partial G$ as the only di-critical vertices. In step 2 this orientation of $G$ defines unique boundary $Z$- and $S$-Hamiltonian paths $h_0$ and $h_1$ from $\underline{v}$ to $\bar{v}$ in the filled graph $G_2$, which follow the given orientation on the 1-skeleton $G$. In step 3 we define the permutation $\pi := h_0^{-1} \circ h_1$ according to (2.3). By [FiRo07b], $\pi = \pi_f$ is a dissipative Morse meander. The proofs of theorems 1.1 and 1.2 then assert, in the final step 4, that the Sturm attractor associated to $f$ possesses the prescribed design: the 1-skeleton $\mathcal{C}_f^1$ and the connection graph $\mathcal{C}_f$ of the Sturm attractor $\mathcal{A}_f$ coincide with the prescribed 1-skeleton $G$ and its filled counterpart $G_2$, respectively.

## 2.2 Trivial substitution equivalence

The trivial linear substitutions $x \mapsto -x$ and $u \mapsto -u$ into solutions $u(t, \cdot) \in X$ of the PDE (1.1), (1.2) generate an action of the Klein group $\mathbb{Z}_2 \times \mathbb{Z}_2$ on the nonlinearities $f$. They replace $f(x, u, p)$ by $f(-x, u, -p)$ and $-f(x, -u, -p)$, respectively. We call the linearly flow equivalent Sturm attractors $\mathcal{A}_f$ on the same group orbit of substitutions *trivially substitution equivalent*. We also use this terminology for the associated Sturm permutations, connection graphs, and 1-skeletons.

For example, let $(h_0, h_1)$ be a boundary Hamiltonian pair in the plane 1-skeleton $G$. Then the interchanged pair $(h_1, h_0)$ is also a boundary $ZS$-Hamiltonian pair, after a reflection of the plane embedding of $G$ which fixes the boundary extrema $\underline{v}, \bar{v}$ and preserves any orientation of $G$. In the PDE (1.1), (1.2) this corresponds to the substitution $x \mapsto -x$; see (2.2). By (2.3) this amounts to replacing the Sturm permutation $\pi = h_0^{-1} \circ h_1$ by its inverse $\pi^{-1} = h_1^{-1} \circ h_0$. Similarly, we may reverse the orientation of $G$ and interchange the extrema $\underline{v}, \bar{v}$ by the substitution $u \mapsto -u$ in the PDE (1.1), (1.2). This rotates the plane embedding of $G$ by 180 degrees, and amounts to replacing $h_j$ by the reverse paths $h_j^- := h_j \kappa$, with the involution $\kappa$ defined as

$$(2.7) \qquad\qquad \kappa(j) = N + 1 - j,$$

for $j = 1, \ldots, N$. The $ZS$ parity of the paths is preserved, and $\pi$ is replaced by its conjugate $\kappa \pi \kappa$.

12
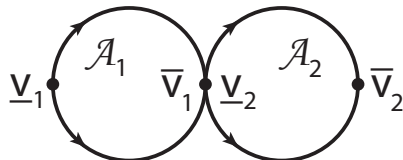
Figure 2.2: Trivial stacking of Sturm attractors $\mathcal{A}_j$ and their connection graphs $G_{2,j} = \mathcal{C}_j$ via $\bar{v}_1 = \underline{v}_2$.

Therefore the two trivial substitutions above indeed generate an action of the Klein group $\mathbb{Z}_2 \times \mathbb{Z}_2$ on the Sturm permutations. Below, we usually represent each such group orbit by only a single instance.

## 2.3 Attractor stacking

For practical computations of Sturm permutations we mention *stacking* as one building principle for Sturm attractors. For $j = 1, 2$, let $\mathcal{A}_j$ denote Sturm attractors with connection graphs $G_{2,j} = \mathcal{C}_j$ and with extremal equilibria $\underline{v}_j$, $\bar{v}_j$. Let $\mathcal{C}$ be the union of $\mathcal{C}_1$ and $\mathcal{C}_2$ with $\bar{v}_1$ and $\underline{v}_2$ identified, i.e.,

$$(2.8) \qquad\qquad \mathcal{C} = (\mathcal{C}_1 \cup \mathcal{C}_2)/\{\bar{v}_1 = \underline{v}_2\}$$

In other words, $v = \bar{v}_1 = \underline{v}_2$ is a cut-vertex of $G_2$. Then $\mathcal{C}$ is again the connection graph $\mathcal{C}_f$ of a Sturm attractor $\mathcal{A}_f$, by theorem 1.1. Indeed the respective orientations of the 1-skeletons $\mathcal{C}_1^1$, $\mathcal{C}_2^1$ fit together, at $v$, without making $v$ di-critical. Also note $\underline{v} = \underline{v}_1$ and $\bar{v} = \bar{v}_2$ for $\mathcal{C}$.

On the level of boundary $ZS$-Hamiltonian pairs $(h_0^j, h_1^j)$, stacking simply amounts to traversing the paths $h_\iota^1$ and $h_\iota^2$ successively. Similarly we may simply attach the shooting curve $\mathcal{S}_2$ of $\pi_2$ to the right of $\mathcal{S}_1$, $\pi_1$ and thus obtain $\mathcal{S}$ and $\pi$ for $\mathcal{A}$ and $\mathcal{C}$.

On the level of nonlinearities $f$ and $f_j$ attractor stacking can be performed quite explicitly. We first normalize $f_j$ such that $\underline{v}_j$, $\bar{v}_j$ become $x$-independent equilibria,

$$(2.9) \qquad\qquad f_j(x, u, p) \equiv 0 \ \text{ for } \ u = \underline{v}_j, \bar{v}_j \in \mathbb{R},$$

with identical first and second $u$-derivatives at $u = v := \bar{v}_1 = \underline{v}_2$ and for all real $p$. This can be achieved, without perturbing any of the other equilibria, and without affecting $\bar{v}_1$, $\underline{v}_2$ being sinks. In particular it keeps the Sturm permutations $\pi_j = \pi_{f_j}$ fixed, and does not affect the connection graphs. We then stack $f_j$ to become a $C^2$-function

$$(2.10) \qquad\qquad f(x, u, p) := \begin{cases} f_1(x, u, p), & \text{for } u < v, \\ f_2(x, u, p), & \text{for } u \geq v. \end{cases}$$

By this construction, the connection graph $\mathcal{C}_f$ coincides with the trivial stacking of $\mathcal{C}_{f1}$ and $\mathcal{C}_{f2}$. Indeed connections within $\mathcal{C}_{f_j}$ are unaffected, by the monotonicity principle, and heteroclinic connections between $\mathcal{C}_{f_1}$ and $\mathcal{C}_{f_2}$ are blocked by $v$.

## 2.4 Duality

In [FiRo07a] we have introduced a slight variant $G^*$ of the standard *dual graph* of $G$. Vertices of $G^*$ inside $\partial G$ are the Morse sources of the filled graph $G_2$ in the bounded faces of $G$. We replace the single vertex of the standard dual, representing the unbounded exterior face of $\partial G$, by two vertices $\underline{v}^*$, $\bar{v}^*$ as follows. Edges $e^*$ of $G^*$ connect Morse sources of adjacent faces of $G$. Here distinct (bounded or unbounded) faces are called adjacent if their boundaries share at least one edge. We orient edges $e^*$, based on the oriented edge $e$ which the adjacent faces share, such that the ordered pair $(e^*, e)$ is oriented positively at the bisecting Morse saddle $\{v\} = e \cap e^*$. Then $\bar{v}^*$ terminates all edges $e^*$ which point away from $\partial G$, to the outside, whereas $\underline{v}^*$ provides a start vertex for all edges $e^*$ pointing toward $\partial G$ from the outside. By lemma 2.2 in [FiRo07a] this construction is possible in the plane without producing intersecting edges of $G^*$. For examples see figures 2.3, 3.6, and sections 2.5, 3, 4 below.

The following elementary observations hold for our duality construction. Let $G^-$ denote the graph $G$ with all orientations reversed. Then

$$(2.11) \qquad\qquad (G^-)^* \;=\; (G^*)^-;$$

$$(2.12) \qquad\qquad G^{**} \;=\; G^- \,.$$

Under the assumptions of theorem 1.1 on $G$ or, equivalently, on the undirected dual $G^*$, the filled dual graph $G_2^*$ possesses a boundary $ZS$-Hamiltonian pair $(h_0^*, h_1^*)$ between $\underline{v}^*$ and $\bar{v}^*$ if, and only if, $G_2$ possesses such a pair between $\underline{v}$ and $\bar{v}$.

The above duality induces isomorphisms

$$(2.13) \qquad\qquad \begin{aligned} Z\mathcal{H}_{\underline{v},\bar{v}}(G_2) &\;\rightarrow\; Z\mathcal{H}_{\underline{v}^*,\bar{v}^*}(G_2^*) \\ S\mathcal{H}_{\underline{v},\bar{v}}(G_2) &\;\rightarrow\; S\mathcal{H}_{\underline{v}^*,\bar{v}^*}(G_2^*) \end{aligned}$$

of boundary $ZS$-Hamiltonian pairs in the filled graphs $G_2$ and $G_2^*$. The isomorphism

$$(2.14) \qquad\qquad \begin{aligned} Z\mathcal{H}_{\underline{v},\bar{v}}(G_2) &\;\rightarrow\; S\mathcal{H}_{\underline{v}^*,\bar{v}^*}(G_2^*) \\ h_0 &\;\mapsto\; h_1^* \end{aligned}$$

14
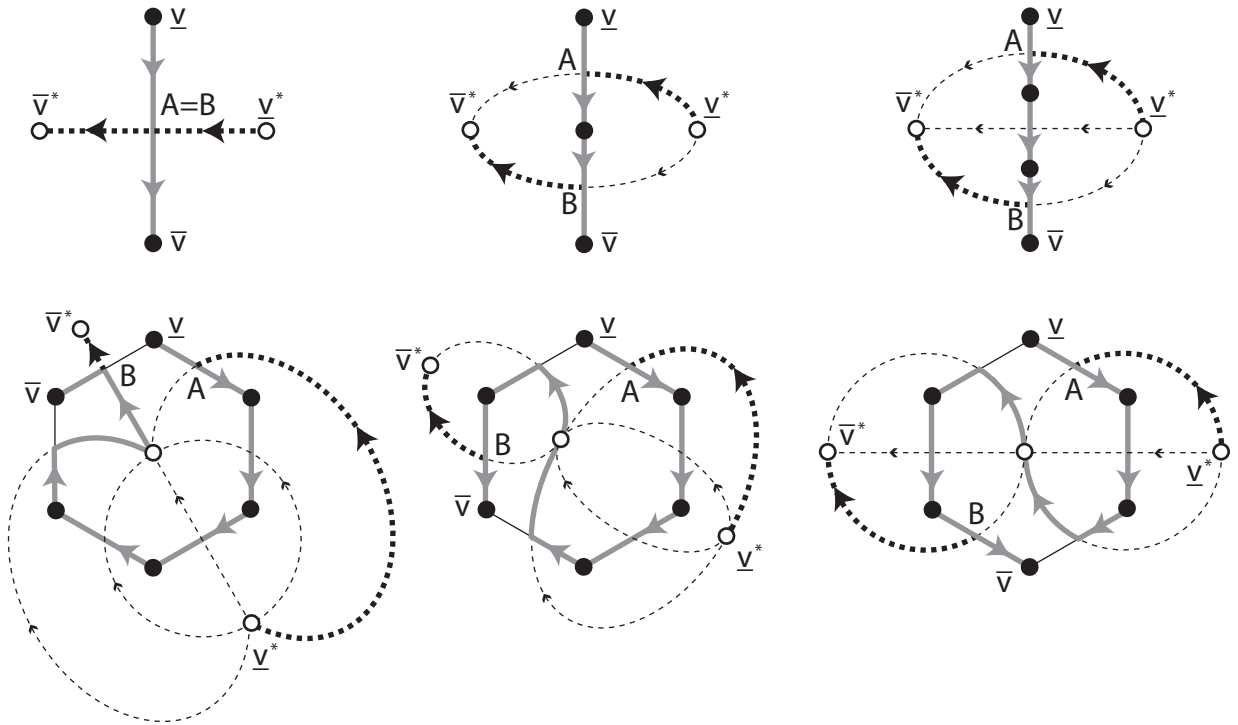
Figure 2.3: Some examples of oriented graph duals $G^*$ (dashed) of $G$ (solid), and $Z$-Hamiltonian paths in $G^d$ (gray solid) versus $S$-Hamiltonian paths in $G^*$ (black dashed).

is in fact easily described. Simply replace the first edge $\underline{v}A$ and the last edge $B\bar{v}$, only, of a $Z$-Hamilton path

$$(2.15) \qquad h_0 = \underline{v}A \ldots B\bar{v} \ \in Z\mathcal{H}_{\underline{v},\bar{v}}(G_2)$$

by their counterparts $\underline{v}^*A$ and $B\bar{v}^*$, respectively:

$$(2.16) \qquad h_1^* = \underline{v}^*A \ldots B\bar{v}^*.$$

See figure 2.3. Similarly, we obtain the mirrored isomorphism

$$(2.17) \qquad \begin{aligned} S\mathcal{H}_{\underline{v},\bar{v}}(G_2) &\rightarrow Z\mathcal{H}_{\underline{v},\bar{v}^*}(G_2^*) \\ h_1 &\mapsto h_0^* \end{aligned}$$

reversing the orientation of $h_1$ and replacing the first and last arcs from/to $\underline{v}, \bar{v}$ by their $\bar{v}^*, \underline{v}^*$ counterparts.

The algebraic description of the dual paths $h_j^*$ and the dual permutation $\pi^* = (h_0^*)^{-1} \cdot h_1^*$ from $h_0$, $h_1$, $\pi$ is also straightforward. In the shared part

$$(2.18) \qquad G_2 \cap G_2^* = G_2 \backslash \{\underline{v}, \bar{v}\} = G_2^* \backslash \{\underline{v}^*, \bar{v}^*\},$$

of the filled graphs, where $G_2$ and $G_2^*$ coincide, the paths $h_0$ and $h_1^*$ also coincide, whereas $h_1$ and $h_0^*$ run in opposite directions. The vertices $\underline{v}, \bar{v}$ are replaced by $\underline{v}^*, \bar{v}^*$, but keep their original neighbors along these paths. Using the same vertex labels for $\underline{v}, \underline{v}^*$, and for $\bar{v}, \bar{v}^*$, respectively, we see that

$$(2.19) \qquad h_0^* = h_1\hat{\kappa}, \quad h_1^* = h_0,$$

where the involution $\hat{\kappa}$ fixes the indices 1 and $N$, in contrast to $\kappa$ from (2.7):

$$(2.20) \qquad \hat{\kappa} = \kappa \circ (1 \ N) = (1 \ N) \circ \kappa = (1, N-1, \ldots, 2, N).$$

Therefore the Sturm permutation $\pi^*$ of the dual graph $\mathcal{C}^*$ satisfies

$$(2.21) \qquad \pi^* = \hat{\kappa}\pi^{-1}.$$

The double dual

$$(2.22) \qquad \pi^{**} = \kappa\pi\kappa$$

is substitution equivalent to $\pi$ by the trivial substitution $v \mapsto -v$ of section 2.2, which reverses the orientations of $\mathcal{C}^1 = G$ and of $\mathcal{C} = G_2$.

In view of theorems 1.1 and 1.2, the isomorphisms (2.13) provide somewhat unexpected "dualities" $\pi \leftrightarrow \pi^*$, $f \leftrightarrow f^*$, $\mathcal{A} \leftrightarrow \mathcal{A}^* := \mathcal{A}_{f^*}$ between Sturm permutations, nonlinearities, and their planar Sturm attractors.
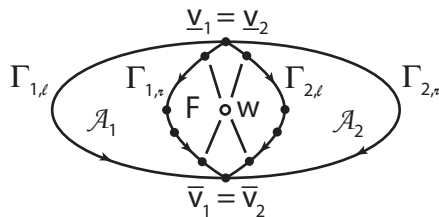
Figure 2.4: Face gluing of attractors $\mathcal{A}_1$, $\mathcal{A}_2$.

## 2.5 Face gluing

We briefly address the dual operation of stacking: face gluing. Consider attractors $\mathcal{A}_j$ and connection graphs $\mathcal{C}_j$ with extrema $\underline{v}_j$, $\bar{v}_j$ and left, right boundaries $\Gamma_{j,\ell}$, $\Gamma_{j,r}$ from $\underline{v}_j$ to $\bar{v}_j$. Let $\mathcal{C}$ consist of $\mathcal{C}_1$, $\mathcal{C}_2$ and a new face $F$ with Morse source $w$ such that the boundaries of the face $F$ coincide with $\Gamma_{1,r}$, $\Gamma_{2,\ell}$ and $\underline{v} = \underline{v}_1 = \underline{v}_2$, $\bar{v} = \bar{v}_1 = \bar{v}_2$ are identified. By the above duality construction the dual 1-skeleton $(\mathcal{C}^1)^*$ is the stacking of the duals $(\mathcal{C}_j^1)^*$ via $\underline{v}_1^* = \bar{v}_2^* = w$. Since duals of connection graphs are connection graphs, and $G^{**} = -G$, the face gluing of $\mathcal{C}_1$ and $\mathcal{C}_2$ via $F$ again produces a connection graph $\mathcal{C}$ with $\underline{v} = \underline{v}_1 = \underline{v}_2$ and $\bar{v} = \bar{v}_1 = \bar{v}_2$. The face gluing operator on the level of nonlinearities however, is far from obvious.

We skip the details of the construction of $h_0, h_1$, and $\pi$ for $\mathcal{C}$, $\mathcal{A}$, in the particular case of face gluing. As a frequent example we just mention that plane oriented 1-skeletons $G$ with adjacent boundary extrema are trivially face glued, with one of the glued components being an $n$-gon attractor.

## 2.6 Example: $n$-gon attractors

Following section 3 in [FiRo07b] we briefly summarize the structure of the general $n$-gon attractors $\mathcal{A}_{n,m}$ for $1 \leq m < n$. See figure 2.5 for the general cases $\mathcal{A}_{n,n-1}$ and $\mathcal{A}_{n,n-[n/2]}$ where $[\cdot]$ denotes the floor function. The $n$-gon attractors $\mathcal{A}_{n,m}$ are all $C^0$ orbit equivalent, for fixed $n$. Their connection graphs $\mathcal{C}_{n,m}$ and 1-skeletons $\mathcal{C}_{n,m}^1$ are isomorphic. But $\mathcal{C}_{n,m}^1$ and $\mathcal{C}_{n,m'}^1$ are neither orientation isomorphic nor substitution equivalent, for $m \neq m'$, unless $m + m' = n$. The same statement holds for trivial substitution equivalence of $\mathcal{A}_{n,m}$ and $\mathcal{A}_{n,m'}$.

The 1-skeleton $G$ of the $n$-gon is a regular plane $n$-gon with Morse sink vertices $v_k$ labeled $k = 1, 3, \ldots, 2n - 1$, clockwise. The filled graph $G_2$ possesses the additional Morse saddles $2k$ bisecting the edges $\{2k - 1, 2k + 1\}$, for $1 \leq k < n$, and the edge $\{2n - 1, 1\}$ for $k = n$. The barycenter of the $n$-gon is the Morse source $2n + 1$ of $G_2$, connected by edges to each
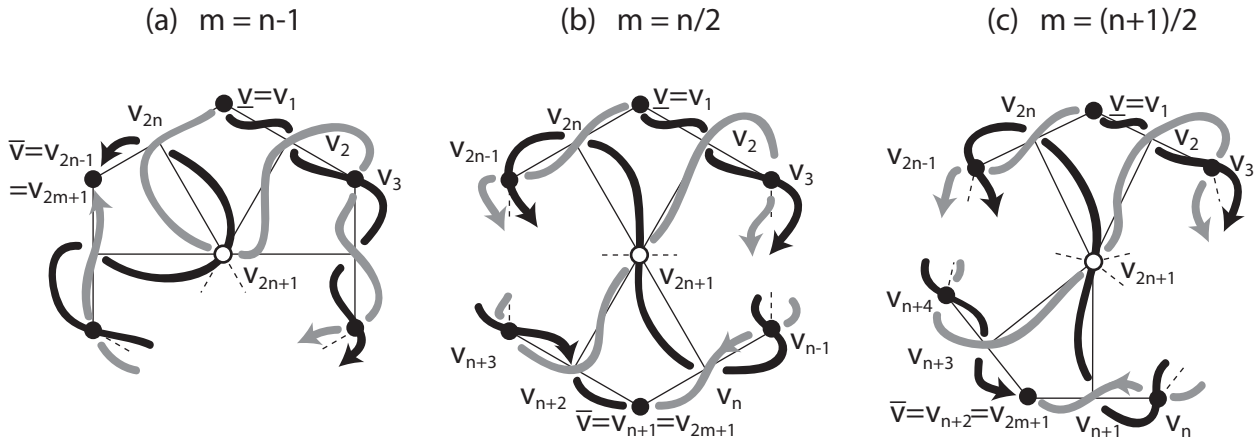
Figure 2.5: The $n$-gon attractors $\mathcal{A}_{n,m}$ with (a) $m = n-1$; (b) $n$ even and $m = n/2$; (c) $n$ odd and $m = (n+1)/2$. $Z$-Hamiltonian path $h_0$ (solid) and $S$-Hamiltonian path $h_1$ (gray)
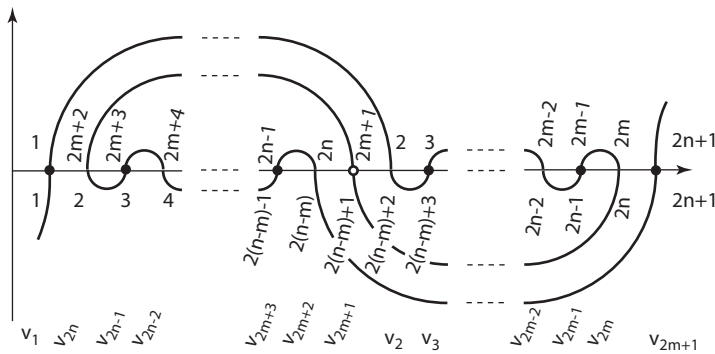


Figure 2.6: Shooting curve and Morse indices of $\pi_{n,m}$. Below axis: $k$; above axis: $\pi_{n,m}(k)$. Labels $k$ above and below axis indicate equilibrium $v_{h_0(k)}$ and $v_{h_1(k)}$ in figure 2.5, respectively.

Morse saddle. Obviously there is only one bounded face $F$: the interior of the $n$-gon. The boundary $\partial F$ is the 1-skeleton $G$.

To design the associated $n$-gon Sturm attractor we follow the recipe at the end of section 2.1: from orientations via $ZS$-Hamiltonian pairs and Sturm permutations to Sturm attractors. The loop-free orientations of $G$, without di-sources and di-sinks other than the Morse sinks $\underline{v}$ and $\bar{v}$, are characterized by the positions of $\underline{v}$ and $\bar{v}$ along the boundary $n$-gon $\partial F$: the two $n$-gon arcs between $\underline{v}$ and $\bar{v}$ are oriented from $\underline{v}$ to $\bar{v}$. Without loss of generality we label

$$(2.23) \qquad\qquad \underline{v} = v_1, \qquad \bar{v} = v_{2m+1}$$

for some $1 \leq m < n$. See figure 2.5 for the unique $ZS$-Hamiltonian paths which result from this orientation.

According to the recipe of section 2.1, the Sturm permutation $\pi = \pi_{n,m}$ is then given by (2.3):

$$(2.24)\, \pi = \begin{pmatrix} 1 & 2 & \dots & 2(n-m) & 2(n-m)+1 & 2(n-m)+2 & \dots & 2n & 2n+1 \\ 1 & 2m+2 & \dots & 2n & 2m+1 & 2 & \dots & 2m & 2n+1 \end{pmatrix}.$$

See figure 2.6 for the associated shooting curve and the Morse indices $i_k$ of $\pi_{n,m}$. This completes the design of all $n$-gon Sturm attractors.

# 3 Specifics: 37 planar Sturm attractors with up to 11 equilibria

We apply theorems 1.1 and 1.2 to enumerate all planar Sturm attractors with up to 11 hyperbolic equilibria, in this section. We eliminate orientation isomorphic duplicates and the trivial substitution equivalences generated by $x \mapsto -x$, and by $v \mapsto -v$; see section 2.2 above. We use the duality pairings of section 2.4 to effectively cut the total number of cases in half.

Except for one indecomposable self-dual case, we do not follow the general design recipe detailed at the end of section 2.1. Instead, we proceed from the $n$-gons of section 2.6 by the attractor stacking and face gluing decompositions of sections 2.3 and 2.5, to inductively exhaust all possibilities.

For each nontrivial example we present the oriented 1-skeleton $G = \mathcal{C}_f^1$ of the connection graph, the oriented dual 1-skeleton $G^* = \mathcal{C}_{f^*}^1$ as introduced in section 2.4, the unique boundary $ZS$-Hamiltonian pair $(h_0, h_1)$, and the associated Sturm permutation $\pi$.

Let $\mu_i$ count the number of equilibria with Morse index $i \in \{0, 1, 2\}$. We then enumerate the 37 connection graphs $\mathcal{C}$ with up to 11 equilibria, and up to trivial substitution equivalences,